

Modelling of Thermo Mechanical Response in Anisotropic Photothermoelastic Plate

Rajneesh Kumar¹

¹ Department of Mathematics, Kurukshetra University, Kurukshetra, Haryana, India.

Nidhi Sharma²

² Department of Mathematics, Maharishi Markandeshwar University Mullana, Ambala, Haryana, India.

Supriya Chopra^{*3}

^{3*} Department of Mathematics, Government College for Women, Ambala city, Haryana, India.

Abstract - The manuscript focused on developing the mathematical model to estimate the response of thermomechanical and carrier density loading in anisotropic photothermoelastic plate. Problem is formulated for a specific type of anisotropy having two planes of symmetry to recover the equations for orthotropic photothermoelastic plate. Laplace and Fourier transform are taken into account to solve the problem and obtain the boundary solution to satisfy the imported boundary conditions. Specific types of loading (uniformly distributed, linearly distributed, concentrated and continuous) are considered to obtain the components of displacement, stress, temperature distribution and carrier density distribution in the new domain. Numerical technique is employed to compute the analytic results and the obtained results are displayed in the form of graphs to show the effects of orthotropy, phase lag and one relaxation time for the resulting quantities. Some degrading results are recovered from the present case.

Keywords : *photothermoelastic orthotropic, Laplace transform, Fourier transform dual phase lag, thermomechanical loading, carrier density loading, uniformly distributed force, linearly distributed force.*

INTRODUCTION

Semiconducting materials have been widely applied in modern engineering applications with the present development of technologies. When a semiconductor surface is exposed to a beam of laser, some electrons will be excited. In this case, the photo-excited free carriers will be produced with non-radiative transitions, and a recombination between electron and hole plasma occurs. Many efforts are made to explore the nature of semiconductors in last few years. The technique adopted is photo acoustic and photo thermal technology.

Photoacoustic (PA) and photothermal (PT) science and technology have extensively developed new methods in the investigation of semiconductors and microelectronic structures during the last few years. PA and PT techniques were recently established as diagnostic methods with good sensitivity to the dynamics of photoexcited carrier. (Mandelis[1], Almond and Patel[2], Mandelis and Michaelian[3]) Photogeneration of electron-hole pairs, i.e., the carriers-diffusion wave or plasma wave, generated by an absorbed intensity modulated laser beam, may, play a dominant role in PA and PT experiments for most semiconductor materials. Depth dependent plasma waves contribute to the generation of periodic heat and mechanical vibrations, i.e., thermal and elastic waves. This mechanism of elastic wave generation is a specific of semiconductors. The electronic deformation mechanism is based on the fact that photogenerated plasma in the semiconductor causes deformation of the crystal lattice, i.e. deformation of the potential of the conduction and valence bands in the semiconductor. Thus, photoexcited carries may cause local strain in the sample. This strain in turn may produce plasma waves in the semiconductor in a manner analogous to thermal wave generation by local periodic elastic deformation. Many problems of deformation and wave propagation problem in a semiconducting medium have become more important academic and applicable value. Many notable researchers have extensively examined various problems in photothermoelastic medium as Abbas[4], Lotfy[5-7], Lotfy et.al.[8], Hobiny and Abbas[9], Jahangir et.al.[10], Zenkour[11], Alzahrani and

Abbas [12,13].

[TareqSaeed\[14\]](#) studied the photo-thermal interactions in semiconductor media by utilizing hyperbolic two-temperature model with one thermal relaxation time. The variations of the carrier density, the thermodynamic, the conductive temperatures, the stress and the displacement in a semi-infinite semiconductor material have been estimated. Abbas et.al.[15] discussed photo-thermal-elastic interactions in an unbounded semiconductor media containing a cylindrical hole under a hyperbolic two-temperature are investigated using the coupled theory of thermo-elasticity and plasma waves. Hobiny et.al. [16] discussed on photo-thermo-elastic wave in a two dimension semi-conductor material caused by ramp-type heating. Alzahrani and Abbas [17] studied the numerical solutions of the thermal damages of biological tissue by nonlinear dual-phase-lag theory under different boundary conditions. Zakaria et.al.[18] deals with the study of photothermoelastic interactions in an isotropic homogeneous semiconductor solid, using a new model of generalized thermoelectricity with a memory-dependent derivative of heat conduction and the governing equations of the system are derived based on the dual-phase lag model (DPL) and the wave equation of coupled plasma. Zakaria et.al.[19] constructed a modified generalized fractional photothermoelastic model on the basis of the fractional calculus technique. Author introduced Fourier law using the Taylor series expansion of higher time-fractional for the considered model.

In this paper, we studied deformation due to thermomechanical and carrier density loading in orthotropic photothermoelastic plate with dual phase lag. Laplace and Fourier transform are employed to solve the problem. The analytical expressions of normal stress, temperature distribution and carrier density distribution are computed in the transformed domain. However, the resulting quantities are obtained in the physical domain by using numerical inversion technique. The variations of normal stress component, temperature distribution and carrier density distribution with distance and thickness of the plate are depicted graphically to demonstrate the effect of orthotropy, phase lag and Lord and Shulman's theory with one relaxation time.

BASIC EQUATIONS

The constitutive relation and the field equations for photothermoelastic with dual phase lag model in absence of body forces, heat sources and carrier photogeneration sources are described by (Tzou [20]; Todorovic [21,22]).

$$t_{ij} = C_{ijkl}e_{kl} - \alpha_{ij}T - \gamma_{ij}N \tag{1}$$

$$C_{ijkl}e_{kl} - \alpha_{ij}T_{,h} - \gamma_{ij}N_{,h} = \rho\ddot{u}_i \tag{2}$$

$$K_{ij} \left(1 + \tau_T \frac{\partial}{\partial t} \right) T_{,ij} = -\frac{E_g}{\tau} N + \left(1 + \tau_q \frac{\partial}{\partial t} + \frac{m_o \tau_q^2}{2} \frac{\partial^2}{\partial t^2} \right) (\rho C_e \dot{T} + T_o \alpha_{ij} e_{ij}) \tag{3}$$

$$D_{ij}^* N_{,ij} = \frac{\partial N}{\partial t} + \frac{N}{\tau} - \delta \frac{T}{\tau} \tag{4}$$

(i, j, k, l, h=1,2,3)

The following cases arise:

(i) The dual phase lag model

$$0 < \tau_T < \tau_q, m_o = 1,$$

(ii) The Lord and Shulman's theory [23]

$$\tau_q = \tau_0 > 0, \tau_T = m_o = 0,$$

(iii) The classical dynamical coupled theory [24]

$$\tau_T = \tau_q = m_o = 0$$

where

τ_T – the phase lag of temperature gradient, τ_q – the phase lag of heat flux, τ_0 – the thermal relaxation time, C_{ijkl} – elastic parameters, α_{ij} – are coefficient of linear thermal expansion, γ_{ij} – coefficient of electronic deformation, u_i – components of displacement, T- the temperature distribution, T_o – the reference

temperature, $N = n - n_0$, n_0 - equilibrium carrier concentration, E_g - the semiconductor energy gap, ρ - the medium density, t_{ij} - the components of stress tensor, K_{ij} - thermal conductivity, C_e - the specific heat, $\delta = \frac{\partial n_0}{\partial T}$ the thermal activation coupling parameter, τ - the photogenerated carrier lifetime, t - the time variable, D_{ij}^* - the coefficients of carrier diffusion, e_{kl} - the components of elastic strain.

PROBLEM STATEMENT

Consider an infinite orthotropic phototheroelastic plate with dual phase lag of finite thickness $2d$. A plate is homogeneous, isotropic and thermal conducting with initial uniform temperature T_0 . The middle plane of the plate coincide with $x_1 - x_2$ plane such that $-d \leq x_3 \leq d$ and $-\infty < x_1, x_2 < \infty$, the origin of the coordinate system is taken at any point of the middle plane. The boundary surface $x_3 = \pm d$ is subjected to thermomechanical and carrier density loading. Let the $x_1 - x_3$ plane be taken as the plane of incidence and restrict our analysis to this plane, so that the physical field variables are function of x_1, x_3, t . Thus, the displacement components, temperature distribution and carrier density distribution are given by

$$\mathbf{u} = (u_1(x_1, x_3, t), 0, u_3(x_1, x_3, t)), T = T(x_1, x_3, t) \text{ and } N = N(x_1, x_3, t) \quad (5)$$

We have used appropriate plane of symmetry, following (Slaughter[25]) on the set of equations (1) to (4) to derive the equations for orthotropic photothermoelastic solid for two dimensional problem with the aid of equation (5), take the following forms

$$C_{11} \frac{\partial^2 u_1}{\partial x_1^2} + C_{55} \frac{\partial^2 u_1}{\partial x_3^2} + (C_{13} + C_{55}) \frac{\partial^2 u_3}{\partial x_1 \partial x_3} - \alpha_1 \frac{\partial T}{\partial x_1} - \gamma_1 \frac{\partial N}{\partial x_1} = \rho \frac{\partial^2 u_1}{\partial t^2} \quad (6)$$

$$C_{55} \frac{\partial^2 u_3}{\partial x_1^2} + C_{33} \frac{\partial^2 u_3}{\partial x_3^2} + (C_{13} + C_{55}) \frac{\partial^2 u_1}{\partial x_1 \partial x_3} - \alpha_3 \frac{\partial T}{\partial x_3} - \gamma_3 \frac{\partial N}{\partial x_3} = \rho \frac{\partial^2 u_3}{\partial t^2} \quad (7)$$

$$K_1 \left(1 + \tau_T \frac{\partial}{\partial t} \right) \frac{\partial^2 T}{\partial x_1^2} + K_3 \left(1 + \tau_T \frac{\partial}{\partial t} \right) \frac{\partial^2 T}{\partial x_3^2} = -\frac{E_g}{\tau} N + \left(1 + \tau_q \frac{\partial}{\partial t} + \frac{m_0 \tau_q^2}{2} \frac{\partial^2}{\partial t^2} \right) \left(\rho C_e \frac{\partial T}{\partial t} + T_0 \left(\alpha_1 \frac{\partial^2 u_1}{\partial x_1 \partial t} + \alpha_3 \frac{\partial^2 u_3}{\partial x_3 \partial t} \right) \right) \quad (8)$$

$$D_1^* \frac{\partial^2 N}{\partial x_1^2} + D_3^* \frac{\partial^2 N}{\partial x_3^2} = \frac{\partial N}{\partial t} + \frac{N}{\tau} - \delta \frac{T}{\tau} \quad (9)$$

$$t_{33} = C_{13} \frac{\partial u_1}{\partial x_1} + C_{33} \frac{\partial u_3}{\partial x_3} - \alpha_3 T - \gamma_3 N \quad (10)$$

$$t_{31} = C_{55} \left(\frac{\partial u_1}{\partial x_3} + \frac{\partial u_3}{\partial x_1} \right) \quad (11)$$

$$t_{11} = C_{11} \frac{\partial u_1}{\partial x_1} + C_{13} \frac{\partial u_3}{\partial x_3} - \alpha_1 T - \gamma_1 N \quad (12)$$

where

$$\alpha_1 = C_{11} \alpha_1^* + C_{12} \alpha_2^* + C_{13} \alpha_3^*, \alpha_3 = C_{13} \alpha_1^* + C_{23} \alpha_2^* + C_{33} \alpha_3^*,$$

$$\gamma_1 = C_{11} \gamma_1^* + C_{12} \gamma_2^* + C_{13} \gamma_3^*, \gamma_3 = C_{13} \gamma_1^* + C_{23} \gamma_2^* + C_{33} \gamma_3^*$$

γ_1^*, γ_2^* and γ_3^* are linear thermal expansion coefficients, γ_1^*, γ_2^* and γ_3^* are electronic deformation coefficients, K_1, K_3 - thermal conductivity and D_1^* and D_3^* are carrier diffusion coefficients.

To facilitate the solution, we introduce the following dimensionless quantities

$$(x'_1, x'_3, u'_1, u'_3) = \eta_1 c_0 (x_1, x_3, u_1, u_3), (t'_{11}, t'_{33}, t'_{31}) = \frac{1}{c_{11}} (t_{11}, t_{33}, t_{31}), (t', \tau'_T, \tau'_q) = \eta_1 c_0^2 (t, \tau_T, \tau_q)$$

$$T' = \frac{\alpha_1 T}{\rho c_0^2}, \tau' = \eta_1 c_0^2 \tau, N' = \frac{N}{n_0} \quad (13)$$

where

$$\eta_1 = \frac{\rho C_E}{K_1}, c_0^2 = \frac{C_{11}}{\rho}$$

By taking into consideration equation (13), reduce the equations (6)-(12) and suppressing the prime yield

$$\frac{\partial^2 u_1}{\partial x_1^2} + g_1 \frac{\partial^2 u_1}{\partial x_3^2} + g_2 \frac{\partial^2 u_3}{\partial x_1 \partial x_3} - \frac{\partial T}{\partial x_1} - g_3 \frac{\partial N}{\partial x_1} = \frac{\partial^2 u_1}{\partial t^2} \quad (14)$$

$$\frac{\partial^2 u_3}{\partial x_1^2} + g_4 \frac{\partial^2 u_3}{\partial x_3^2} + g_5 \frac{\partial^2 u_1}{\partial x_1 \partial x_3} - g_6 \frac{\partial T}{\partial x_3} - g_7 \frac{\partial N}{\partial x_3} = g_8 \frac{\partial^2 u_3}{\partial t^2} \quad (15)$$

$$\left(1 + \tau_T \frac{\partial}{\partial t}\right) \frac{\partial^2 T}{\partial x_1^2} + k^* \left(1 + \tau_T \frac{\partial}{\partial t}\right) \frac{\partial^2 T}{\partial x_3^2} = g_{11} \frac{N}{\tau} + \left(1 + \tau_q \frac{\partial}{\partial t} + \frac{m_0 \tau_q^2}{2} \frac{\partial^2}{\partial t^2}\right) \left(g_{12} \frac{\partial T}{\partial t} + g_{13} \frac{\partial^2 u_1}{\partial x_1 \partial t} + g_{14} \frac{\partial^2 u_3}{\partial x_3 \partial t}\right) \quad (16)$$

$$\frac{\partial^2 N}{\partial x_1^2} + D^* \frac{\partial^2 N}{\partial x_3^2} = g_9 \frac{\partial N}{\partial t} + g_9 \frac{N}{\tau} - g_{10} \frac{T}{\tau} \quad (17)$$

$$t_{33} = g_{15} \frac{\partial u_1}{\partial x_1} + g_{16} \frac{\partial u_3}{\partial x_3} - g_{17} T - g_{18} N \quad (18)$$

$$t_{31} = g_1 \left(\frac{\partial u_1}{\partial x_3} + \frac{\partial u_3}{\partial x_1}\right) \quad (19)$$

$$t_{11} = \frac{\partial u_1}{\partial x_1} + g_{15} \frac{\partial u_3}{\partial x_3} - T - g_3 N \quad (20)$$

where

$$g_1 = \frac{C_{55}}{C_{11}}, g_2 = \frac{C_{13} + C_{55}}{C_{11}}, g_3 = \frac{\gamma_1 n_0}{C_{11}}, g_4 = \frac{C_{33}}{C_{55}}, g_5 = \frac{C_{13} + C_{55}}{C_{55}}, g_6 = \frac{\alpha_3 C_{11}}{\alpha_1 C_{55}}, g_7 = \frac{\gamma_3 n_0}{C_{55}}, g_8 = \frac{C_{11}}{C_{55}},$$

$$g_9 = \frac{1}{\eta_1 D_1^*}, g_{10} = \frac{\delta \rho C_0^2}{\alpha_1 D_1^* n_0 \eta_1}, g_{11} = -\frac{E_g n_0 \alpha_1}{K_1 \eta_1 \rho C_0^2}, g_{12} = \frac{\rho C_E}{K_1 \eta_1}, g_{13} = \frac{T_0 \alpha_1 \alpha_1}{K_1 C_{11} \eta_1}, g_{14} = \frac{T_0 \alpha_3 \alpha_1}{K_1 \eta_1 C_{11}},$$

$$g_{15} = \frac{C_{13}}{C_{11}}, g_{16} = \frac{C_{33}}{C_{11}}, g_{17} = \frac{\alpha_3}{\alpha_1}, g_{18} = \frac{\gamma_3 n_0}{C_{11}}, k^* = \frac{k_3}{k_1}, D^* = \frac{D_3}{D_1} \quad (21)$$

Now, Laplace transform of a function $f(x_1, x_3, p)$ w.r.t. time variable 't' and 'p' is Laplace transform variable defined as

$$\bar{f}(x_1, x_3, p) = \mathcal{L}\{f(x_1, x_3, p)\} = \int_0^\infty f(x_1, x_3, p) e^{-pt} dt \quad (22)$$

The Fourier transform for the function $f(x_1, x_3, p)$ take the form and ξ is Fourier transform variable

$$\hat{f}(x_1, x_3, p) = \mathcal{F}\{f(x_1, x_3, p)\} = \int_{-\infty}^\infty f(x_1, x_3, p) e^{i\xi x_1} dx_1 \quad (23)$$

Employing Laplace and Fourier transform given by equations (22)-(23) on equations (14)-(19), reduce the system of differential equations as:

$$-\xi^2 \hat{u}_1 + g_1 \frac{d^2 \hat{u}_1}{dx_3^2} + g_2 i\xi \frac{d\hat{u}_3}{dx_3} - i\xi \hat{T} - i\xi g_3 \hat{N} = p^2 \hat{u}_1 \quad (24)$$

$$-\xi^2 \hat{u}_3 + g_4 \frac{d^2 \hat{u}_3}{dx_3^2} + g_5 i\xi \frac{d\hat{u}_1}{dx_3} - g_6 \frac{d\hat{T}}{dx_3} - g_7 \frac{d\hat{N}}{dx_3} = g_8 p^2 \hat{u}_3 \quad (25)$$

$$-(1 + p\tau_T)\xi^2 \hat{T} + k^*(1 + p\tau_T) \frac{d^2 \hat{T}}{dx_3^2} = g_{11} \frac{\hat{N}}{\tau} + \left(1 + p\tau_q + p^2 \frac{m_0 \tau_q^2}{2}\right) \left(g_{12} p \hat{T} + g_{13} p \frac{d\hat{u}_1}{dx_1} + g_{14} p \frac{d\hat{u}_3}{dx_3}\right) \quad (26)$$

$$-\xi^2 \hat{N} + D^* \frac{d^2 \hat{N}}{dx_3^2} = g_9 p \hat{N} + g_9 \frac{\hat{N}}{\tau} - g_{10} \frac{\hat{T}}{\tau} \quad (27)$$

$$\hat{t}_{33} = g_{15} i\xi \hat{u}_1 + g_{16} \frac{d\hat{u}_3}{dx_3} - g_{17} \hat{T} - g_{18} \hat{N} \quad (28)$$

$$\hat{t}_{31} = g_1 \left(\frac{d\hat{u}_1}{dx_3} + i\xi \hat{u}_3\right) \quad (29)$$

After some algebraic simplification equations (24)-(27) yield

$$(D^8 + R_1 D^6 + R_2 D^4 + R_3 D^2 + R_4)(\hat{u}_1, \hat{u}_3, \hat{T}, \hat{N}) = 0 \quad (30)$$

Where

$$R_1 = \frac{r_{15}}{r_{14}}, R_2 = \frac{r_{16}}{r_{14}}, R_3 = \frac{r_{17}}{r_{14}}, R_4 = \frac{r_{18}}{r_{14}}$$

$$r_{14} = -g_1 g_4 r_9 D^*$$

$$r_{15} = r_{10} g_1 g_4 D^* + r_6 r_9 g_1 D^* - g_1 g_6 r_8 D^* + r_1 g_4 r_9 D^* + g_1 g_4 r_9 r_{13} + r_2 r_5 r_9 D^*$$

$$r_{16} = -r_{11} r_{12} g_4 g_1 + g_7 g_1 r_{12} r_8 - r_1 g_4 r_{10} D^* - r_1 r_6 r_9 D^* + g_6 r_1 r_8 D^* - g_4 g_1 r_{10} r_{13} - r_9 g_1 r_6 r_{13} \\ + g_6 g_1 r_8 r_{13} - g_4 r_1 r_9 r_{13} - r_2 r_5 r_{10} D^* + r_2 g_6 r_7 D^* - r_2 r_9 r_5 r_{13} + r_3 r_8 r_5 D^* - r_3 g_4 r_7 D^* \\ - r_6 g_1 r_{10} D^*$$

$$r_{17} = r_{11} r_{12} r_6 r_{12} + r_1 r_{12} r_{12} g_4 - r_{12} r_1 r_8 g_7 + r_2 r_{11} r_5 r_{12} - r_7 r_2 g_7 r_{12} - r_4 r_8 r_5 r_{12} + r_4 g_4 r_7 r_{12} + r_1 r_6 r_{10} D^* + \\ r_6 r_{10} r_{13} g_1 + r_1 g_4 r_{10} r_{13} + r_1 r_6 r_9 r_{13} - r_1 g_6 r_8 r_{13} + r_2 r_5 r_{10} r_{13} - r_2 g_6 r_7 r_{13} + r_3 r_7 r_6 D^* -$$

$$r_3 r_8 r_5 r_{13} + r_3 r_7 g_4 r_{13}$$

$$r_{18} = -r_1 r_{11} r_6 r_{12} - r_4 r_7 r_6 r_{12} - r_1 r_{10} r_6 r_{13} - r_3 r_7 r_6 r_{13} \quad (31)$$

The general solution of eq. (31) is written as

$$(\widehat{u}_1, \widehat{u}_3, \widehat{T}, \widehat{N}) = \sum_{j=1}^4 (1, \alpha_{1j}, \beta_{1j}, \gamma_{1j}) C_j \cosh m_j x_3 \quad (32)$$

Where

$m_j (j = 1, 2, 3, 4)$ are roots of $D^8 + R_1 D^6 + R_2 D^4 + R_3 D^2 + R_4 = 0$, and coupling parameters are

$$\alpha_{1j} = \sum_{j=1}^4 \frac{R_9 m_j^5 + R_{10} m_j^3 + R_{11} m_j}{R_5 m_j^6 + R_6 m_j^4 + R_7 m_j^2 + R_8} \quad (33)$$

$$\beta_{1j} = \sum_{j=1}^4 \frac{R_{12} m_j^4 + R_{13} m_j^2 + R_{14}}{R_5 m_j^6 + R_6 m_j^4 + R_7 m_j^2 + R_8} \quad (34)$$

$$\gamma_{1j} = \sum_{j=1}^4 \frac{R_{15} m_j^2 + R_{16}}{R_5 m_j^6 + R_6 m_j^4 + R_7 m_j^2 + R_8} \quad (35)$$

Where

$$R_5 = g_4 r_9 D^* ch_j^3, R_6 = -D^* g_4 r_{10} ch_j^3 - D^* r_4 r_9 ch_j^3 - g_4 r_{13} r_9 ch_j^3 + D^* g_6 r_8 sh_j^2 ch_j$$

$$R_7 = r_{12} r_{11} g_4 ch_j^3 - g_7 r_{12} r_8 sh_j^2 ch_j + D^* r_4 r_{10} - g_4 r_{13} r_{10} ch_j^3 - r_4 r_{13} r_9 ch_j^3 + g_6 r_8 ch_j sh_j^2 - r_{13} g_6 r_8 sh_j^2 ch_j$$

$$R_8 = -r_{12} r_{11} r_4 ch_j^3 + r_{13} r_{10} r_4 ch_j^3, R_9 = D^* r_5 r_9 sh_j ch_j^2$$

$$R_{10} = r_5 D^* r_{10} ch_j^2 sh_j + r_7 D^* g_6 ch_j^2 sh_j - r_5 r_{13} r_9 sh_j ch_j^2$$

$$R_{11} = r_5 r_{12} r_{11} sh_j ch_j^2 - r_7 r_{12} g_7 sh_j ch_j^2 + r_5 r_{13} r_{10} sh_j ch_j^2 - g_6 r_{13} r_7 ch_j sh_j$$

$$R_{12} = r_5 D^* r_8 sh_j^2 ch_j - r_7 D^* g_4 ch_j^3, R_{13} = r_6 D^* r_7 ch_j^3 - r_5 r_{13} r_8 ch_j sh_j^2 + r_7 r_{13} g_4 ch_j^3$$

$$R_{14} = r_6 r_7 r_{13} ch_j^3, R_{15} = r_5 r_{12} r_8 ch_j sh_j^2 - r_7 r_{12} g_4 ch_j^3, R_{16} = r_6 r_{12} r_7 ch_j^3 \quad (36)$$

Expressions for stress components are obtained with the aid of (28), (29) and (32) as

$$\widehat{t}_{33} = g_{15} i \xi \sum_{j=1}^4 C_j \cosh m_j x_3 + g_{16} \sum_{j=1}^4 \alpha_{1j} m_j C_j \sinh m_j x_3 - g_{17} \sum_{j=1}^4 \beta_{1j} C_j \cosh m_j x_3 - \\ g_{18} \sum_{j=1}^4 \gamma_{1j} C_j \cosh m_j x_3 \quad (37)$$

$$\widehat{t}_{31} = (g_1 \sum_{j=1}^4 m_j C_j \sinh m_j x_3 + i \xi g_1 \sum_{j=1}^4 \alpha_{1j} m_j C_j \cosh m_j x_3) \quad (38)$$

BOUNDARY CONDITIONS

The boundary conditions for an orthotropic photothermoelastic plate occupying the plane $x_3 = \pm d$ subjected to normal force, thermal source and carrier density source are considered as

$$\left. \begin{aligned} t_{33} &= -F_1(x_1, t) \\ t_{31} &= 0 \\ T &= F_2(x_1, t) \\ N &= F_3(x_1, t) \end{aligned} \right\} \text{at } x_3 = \pm d \quad (39)$$

Where

$$F_1(x_1, t) = \frac{F_{10} t^2}{16 t_p^2} e^{-t/t_p} \cdot F(x_1) \quad (40)$$

$$F_2(x_1, t) = F_{20} e^{-bx} \cdot H(x_1) \delta(t); \quad (41)$$

$$F_3(x_1, t) = F_{30} \delta(x_1) H(t); \quad (42)$$

for uniformly distributed normal force (UDF), $F(x_1) = F_{10} \begin{cases} 1 & \text{if } |x_1| \leq a \\ 0 & \text{if } |x_1| > a \end{cases}$ (43)

for linearly distributed normal force (LDF), $F(x_1) = F_{10} \begin{cases} 1 - \frac{|x_1|}{a} & \text{if } |x_1| \leq a \\ 0 & \text{if } |x_1| > a \end{cases}$ (44)

also, $H(\cdot)$ is Heaviside step function, $\delta(\cdot)$ is Dirac delta function, F_{10} is the magnitude of the force, F_{20} is the constant temperature applied on the boundary and F_{30} is constant.

Applying Laplace and Fourier transform defined by equations (22)-(23) on equations (39)-(44), we obtain

$$\left. \begin{aligned} \widehat{t}_{33} &= -\widehat{F}_1(\xi, p) \\ \widehat{t}_{31} &= 0 \\ \widehat{T} &= \widehat{F}_2(\xi, p) \\ \widehat{N} &= \widehat{F}_3(\xi, p) \end{aligned} \right\} \quad (45)$$

Where

$$\widehat{F}_1(\xi, p) = \frac{F_{10} t_p}{8 (1+pt_p)^3} \widehat{F}(\xi) \quad (46)$$

$$\widehat{F}_2(\xi, p) = \frac{F_{20}}{b-i\xi} \quad (47)$$

$$\widehat{F}_3(\xi, p) = \frac{F_{30}}{p} \quad (48)$$

for UDF $\widehat{F}(\xi) = \frac{2 \sin \xi a}{\xi}$; $\xi \neq 0$ and for LDF $\widehat{F}(\xi) = \frac{2(1-\cos \xi a)}{\xi^2 a}$; $\xi \neq 0$ (49)

Substituting the values of $\widehat{t}_{33}, \widehat{t}_{31}, \widehat{T}$ and \widehat{N} from equations (37)-(38) and (33), in the transformed boundary condition (45) along with equations (46)-(49) yield

$$\sum_{j=1}^4 (d_j C_j \cosh m_j d) = -\widehat{F}_1(\xi, p) \quad (50)$$

$$\sum_{j=1}^4 (\alpha_j C_j \cosh m_j d) = 0 \quad (51)$$

$$\sum_{j=1}^4 (\beta_j C_j \cosh m_j d) = \widehat{F}_2(\xi, p) \quad (52)$$

$$\sum_{j=1}^4 (\gamma_j C_j \cosh m_j d) = \widehat{F}_3(\xi, p) \quad (53)$$

Where

$$d_j = g_{15} i \xi - g_{17} \beta_{1j} - g_{18} \gamma_{1j} \text{ and } \cosh m_j d = ch_{1j} \quad (j=1,2,3,4)$$

Equation (50)-(53) can be written in matrix form as $AC=B$ (54)

Where

$$A = \begin{bmatrix} d_1 ch_{11} & d_2 ch_{12} & d_3 ch_{13} & d_4 ch_{14} \\ \alpha_{11} ch_{11} & \alpha_{12} ch_{12} & \alpha_{13} ch_{13} & \alpha_{14} ch_{14} \\ \beta_{11} ch_{11} & \beta_{12} ch_{12} & \beta_{13} ch_{13} & \beta_{14} ch_{14} \\ \gamma_{11} ch_{11} & \gamma_{12} ch_{12} & \gamma_{13} ch_{13} & \gamma_{14} ch_{14} \end{bmatrix}, C = \begin{bmatrix} C_1 \\ C_2 \\ C_3 \\ C_4 \end{bmatrix}, B = \begin{bmatrix} -F_1(x_1, t) \\ 0 \\ F_2(x_1, t) \\ F_3(x_1, t) \end{bmatrix} \quad (55)$$

From equation (55), we determine $C_j = \frac{\Delta_j}{\Delta}$, $j = 1,2,3,4$. (56)

Where

$\Delta = \det A$, $\Delta_j =$ determinant of A when j^{th} column of A replaced by B and

$$\begin{aligned} \Delta = & ch_{11}ch_{12}ch_{13}ch_{14} (\alpha_{11}\beta_{12}\gamma_{14}d_3 - \alpha_{11}\beta_{12}\gamma_{13}d_4 - \alpha_{11}\beta_{13}\gamma_{14}d_2 + \alpha_{11}\beta_{13}\gamma_{12}d_4 \\ & + \alpha_{11}\beta_{14}\gamma_{13}d_2 - \alpha_{11}\beta_{14}\gamma_{12}d_3 - \alpha_{12}\beta_{11}\gamma_{14}d_3 + \alpha_{12}\beta_{11}\gamma_{13}d_4 + \alpha_{12}\beta_{13}\gamma_{14}d_1 \\ & + \alpha_{12}\beta_{13}\gamma_{11}d_4 - \alpha_{12}\beta_{14}\gamma_{13}d_1 + \alpha_{12}\beta_{14}\gamma_{11}d_3 + \alpha_{13}\beta_{11}\gamma_{14}d_2 - \alpha_{13}\beta_{11}\gamma_{12}d_4 - \\ & \alpha_{13}\beta_{12}\gamma_{14}d_1 + \alpha_{13}\beta_{12}\gamma_{11}d_4 + \alpha_{13}\beta_{14}\gamma_{12}d_1 - \alpha_{14}\beta_{11}\gamma_{13}d_2 + \alpha_{13}\beta_{14}\gamma_{11}d_2 \\ & + \alpha_{14}\beta_{11}\gamma_{12}d_3 + \alpha_{14}\beta_{12}\gamma_{13}d_1 - \alpha_{14}\beta_{12}\gamma_{11}d_3 - \alpha_{14}\beta_{13}\gamma_{12}d_1 + \alpha_{14}\beta_{13}\gamma_{11}d_2) \end{aligned} \quad (57)$$

$$\Delta_1 = F_1R_{21} + F_2R_{22} - F_3R_{23} \quad (58)$$

$$\Delta_2 = -F_1R_{24} + F_2R_{25} - F_3R_{26} \quad (59)$$

$$\Delta_3 = -F_1R_{27} + F_2R_{28} - F_3R_{29} \quad (60)$$

$$\Delta_4 = -F_1R_{30} + F_2R_{31} - F_3R_{32} \quad (61)$$

and

$$\begin{aligned} R_{21} = & -i\xi ch_{12}ch_{13}ch_{14} (\alpha_{12}\beta_{13}\gamma_{14} - \alpha_{12}\beta_{14}\gamma_{13} - \alpha_{13}\beta_{12}\gamma_{14} + \alpha_{13}\beta_{14}\gamma_{12} + \beta_{12}\gamma_{13} - \alpha_{14}\beta_{13}\gamma_{12}) \\ R_{22} = & -i\xi ch_{11}ch_{12}ch_{14} (\alpha_{11}\beta_{12}\gamma_{14} + \alpha_{11}\beta_{14}\gamma_{12} + \alpha_{12}\beta_{11}\gamma_{14} - \alpha_{12}\beta_{14}\gamma_{11} - \alpha_{14}\beta_{11}\gamma_{12} + \alpha_{14}\beta_{12}\gamma_{11}) \\ R_{23} = & -i\xi ch_{11}ch_{12}ch_{13} (\alpha_{11}\beta_{12}\gamma_{13} - \alpha_{11}\beta_{13}\gamma_{12} - \alpha_{12}\beta_{11}\gamma_{13} - \alpha_{12}\beta_{13}\gamma_{11} - \alpha_{13}\beta_{11}\gamma_{12} + \alpha_{13}\beta_{12}\gamma_{11}) \\ R_{24} = & ch_{14}ch_{12}ch_{13} (-\beta_{12}\gamma_{14}d_3 + \beta_{12}\gamma_{13}d_4 + \beta_{13}\gamma_{14}d_2 - \beta_{13}\gamma_{12}d_4 - \beta_{14}\gamma_{13}d_2 + \beta_{14}\gamma_{12}d_3) \\ R_{25} = & ch_{11}ch_{12}ch_{14} ((\beta_{11}\gamma_{14}d_2 - \beta_{11}\gamma_{12}d_4 - \beta_{12}\gamma_{14}d_1 + \beta_{12}\gamma_{11}d_4 + \beta_{14}\gamma_{12}d_4 - \beta_{14}\gamma_{11}d_2) \\ R_{26} = & ch_{11}ch_{12}ch_{13} (-\beta_{11}\gamma_{13}d_2 + \beta_{11}\gamma_{12}d_3 + \beta_{12}\gamma_{13}d_1 - \beta_{12}\gamma_{11}d_3 - \beta_{13}\gamma_{12}d_1 - \beta_{13}\gamma_{11}d_2) \\ R_{27} = & i\xi ch_{12}ch_{13}ch_{14} (\alpha_{12}\gamma_{14}d_3 - \alpha_{12}\gamma_{13}d_4 - \alpha_{13}\gamma_{14}d_2 + \alpha_{13}\gamma_{12}d_4 + \alpha_{14}\gamma_{13}d_2 - \alpha_{14}\gamma_{12}d_3) \\ R_{28} = & i\xi ch_{11}ch_{12}ch_{14} (-\alpha_{11}\gamma_{14}d_2 + \alpha_{11}\gamma_{12}d_4 + \alpha_{12}\gamma_{14}d_1 - \alpha_{12}\gamma_{11}d_4 - \alpha_{14}\gamma_{12}d_1 + \alpha_{14}\gamma_{11}d_2) \\ R_{29} = & i\xi ch_{11}ch_{12}ch_{13} (\alpha_{11}\gamma_{13}d_2 - \alpha_{11}\gamma_{12}d_3 - \alpha_{12}\gamma_{13}d_1 + \alpha_{12}\gamma_{11}d_3 + \alpha_{13}\gamma_{12}d_1 - \alpha_{13}\gamma_{11}d_2) \\ R_{30} = & i\xi ch_{14}ch_{12}ch_{13} (\alpha_{12}\beta_{13}d_4 - \alpha_{12}\beta_{14}d_3 - \alpha_{13}\beta_{12}d_4 + \alpha_{13}\beta_{14}d_2 + \alpha_{14}\beta_{12}d_3 - \alpha_{14}\beta_{13}d_2) \\ R_{31} = & i\xi ch_{11}ch_{12}ch_{14} (-\alpha_{11}\beta_{12}d_4 + \alpha_{11}\beta_{14}d_2 + \alpha_{12}\beta_{11}d_4 - \alpha_{12}\beta_{14}d_1 - \alpha_{14}\beta_{11}d_2 + \alpha_{14}\beta_{12}d_1) \\ R_{32} = & i\xi ch_{11}ch_{12}ch_{13} (\alpha_{11}\beta_{12}d_3 - \alpha_{11}\beta_{13}d_2 - \alpha_{12}\beta_{11}d_3 + \alpha_{12}\beta_{13}d_1 + \alpha_{13}\beta_{11}d_2 - \alpha_{13}\beta_{12}d_1) \end{aligned} \quad (62)$$

Substituting the values of C_j from equations (56) in equations (32) and (37)-(38), determine the displacement components, stress components, temperature distribution and carrier density distribution as

$$\widehat{u}_1 = \sum_{j=1}^4 C_j \cosh m_j x_3 = \frac{1}{\Delta} (L_1 \widehat{F}_1(\xi, p) + L_2 \widehat{F}_2(\xi, p) + L_3 \widehat{F}_3(\xi, p)) \quad (63)$$

$$\widehat{u}_3 = \sum_{j=1}^4 \alpha_{1j} C_j \cosh m_j x_3 = \frac{1}{\Delta} (L_4 \widehat{F}_1(\xi, p) + L_5 \widehat{F}_2(\xi, p) + L_6 \widehat{F}_3(\xi, p)) \quad (64)$$

$$\widehat{t}_{33} = \sum_{j=1}^4 (d_j \cosh m_j x_3 + e_j \sinh m_j x_3) C_j = \frac{1}{\Delta} (L_{13} \widehat{F}_1(\xi, p) + L_{14} \widehat{F}_2(\xi, p) + L_{15} \widehat{F}_3(\xi, p)) \quad (65)$$

$$\widehat{t}_{31} = \sum_{j=1}^4 (i\xi g_1 \alpha_{1j} \cosh m_j x_3 + g_1 m_j \sinh m_j x_3) C_j = \frac{1}{\Delta} (L_{16} \widehat{F}_1(\xi, p) + L_{17} \widehat{F}_2(\xi, p) + L_{18} \widehat{F}_3(\xi, p)) \quad (66)$$

$$\widehat{T} = \sum_{j=1}^4 \beta_{1j} C_j \cosh m_j x_3 = \frac{1}{\Delta} (L_7 \widehat{F}_1(\xi, p) + L_8 \widehat{F}_2(\xi, p) + L_9 \widehat{F}_3(\xi, p)) \quad (67)$$

$$\widehat{N} = \sum_{j=1}^4 \gamma_{1j} C_j \cosh m_j x_3 = \frac{1}{\Delta} (L_{10} \widehat{F}_1(\xi, p) + L_{11} \widehat{F}_2(\xi, p) + L_{12} \widehat{F}_3(\xi, p)) \quad (68)$$

Where

$$d_j = g_{15} i\xi - g_{17} \beta_{1j} - g_{18} \gamma_{1j}, e_j = g_{16} \alpha_{1j}, \cosh m_j x_3 = ch_j \text{ and } \sinh m_j x_3 = sh_j$$

$$L_1 = R_{21} \cosh m_1 x_3 + R_{24} \cosh m_2 x_3 + R_{27} \cosh m_3 x_3 + R_{30} \cosh m_4 x_3$$

$$L_2 = R_{22} \cosh m_1 x_3 + R_{25} \cosh m_2 x_3 + R_{28} \cosh m_3 x_3 + R_{31} \cosh m_4 x_3$$

$$L_3 = R_{23} \cosh m_1 x_3 + R_{26} \cosh m_2 x_3 + R_{29} \cosh m_3 x_3 + R_{32} \cosh m_4 x_3$$

$$L_4 = \alpha_{11} R_{21} \cosh m_1 x_3 + \alpha_{12} R_{24} \cosh m_2 x_3 + \alpha_{13} R_{27} \cosh m_3 x_3 + \alpha_{14} R_{30} \cosh m_4 x_3$$

$$\begin{aligned}
L_5 &= \alpha_{11}R_{22} \cosh m_1 x_3 + \alpha_{12}R_{25} \cosh m_2 x_3 + \alpha_{13}R_{28} \cosh m_3 x_3 + \alpha_{14}R_{31} \cosh m_4 x_3 \\
L_6 &= \alpha_{11}R_{23} \cosh m_1 x_3 + \alpha_{12}R_{26} \cosh m_2 x_3 + \alpha_{13}R_{29} \cosh m_3 x_3 + \alpha_{14}R_{32} \cosh m_4 x_3 \\
L_7 &= \beta_{11}R_{21} \cosh m_1 x_3 + \beta_{12}R_{24} \cosh m_2 x_3 + \beta_{13}R_{27} \cosh m_3 x_3 + \beta_{14}R_{30} \cosh m_4 x_3 \\
L_8 &= \beta_{11}R_{22} \cosh m_1 x_3 + \beta_{12}R_{25} \cosh m_2 x_3 + \beta_{13}R_{28} \cosh m_3 x_3 + \beta_{14}R_{31} \cosh m_4 x_3 \\
L_9 &= \beta_{11}R_{23} \cosh m_1 x_3 + \beta_{12}R_{26} \cosh m_2 x_3 + \beta_{13}R_{29} \cosh m_3 x_3 + \beta_{14}R_{32} \cosh m_4 x_3 \\
L_{10} &= \gamma_{11}R_{21} \cosh m_1 x_3 + \gamma_{12}R_{24} \cosh m_2 x_3 + \gamma_{13}R_{27} \cosh m_3 x_3 + \gamma_{14}R_{30} \cosh m_4 x_3 \\
L_{11} &= \gamma_{11}R_{22} \cosh m_1 x_3 + \gamma_{12}R_{25} \cosh m_2 x_3 + \gamma_{13}R_{28} \cosh m_3 x_3 + \gamma_{14}R_{31} \cosh m_4 x_3 \\
L_{12} &= \gamma_{11}R_{23} \cosh m_1 x_3 + \gamma_{12}R_{26} \cosh m_2 x_3 + \gamma_{13}R_{29} \cosh m_3 x_3 + \gamma_{14}R_{32} \cosh m_4 x_3 \\
L_{13} &= d_1 \cosh m_1 x_3 + e_1 \sinh m_1 x_3 R_{21} + (d_2 \cosh m_2 x_3 + e_2 \sinh m_2 x_3) R_{24} + (d_3 \cosh m_3 x_3 \\
&+ e_3 \sinh m_3 x_3) R_{27} + (d_4 \cosh m_4 x_3 + e_4 \sinh m_4 x_3) R_{30} \\
L_{14} &= d_1 \cosh m_1 x_3 + e_1 \sinh m_1 x_3 R_{22} + (d_2 \cosh m_2 x_3 + e_2 \sinh m_2 x_3) R_{25} + (d_3 \cosh m_3 x_3 \\
&+ e_3 \sinh m_3 x_3) R_{28} + (d_4 \cosh m_4 x_3 + e_4 \sinh m_4 x_3) R_{31} \\
L_{15} &= (d_1 \cosh m_1 x_3 + e_1 \sinh m_1 x_3) R_{23} + (d_2 \cosh m_2 x_3 + e_2 \sinh m_2 x_3) R_{26} + (d_3 \cosh m_3 x_3 + \\
&e_3 \sinh m_3 x_3) R_{29} + (d_4 \cosh m_4 x_3 + e_4 \sinh m_4 x_3) R_{32} \\
L_{16} &= (i\xi g_1 \alpha_{11} \cosh m_1 x_3 + g_1 m_1 \sinh m_1 x_3) R_{21} + (i\xi g_1 \alpha_{12} \cosh m_2 x_3 + g_1 m_2 \sinh m_2 x_3) R_{24} + \\
&(i\xi g_1 \alpha_{13} \cosh m_3 x_3 + g_1 m_3 \sinh m_3 x_3) R_{27} + (i\xi g_1 \alpha_{14} \cosh m_4 x_3 + g_1 m_4 \sinh m_4 x_3) R_{30} \\
L_{17} &= (i\xi g_1 \alpha_{11} \cosh m_1 x_3 + g_1 m_1 \sinh m_1 x_3) R_{22} + (i\xi g_1 \alpha_{12} \cosh m_2 x_3 + g_1 m_2 \sinh m_2 x_3) R_{25} + \\
&(i\xi g_1 \alpha_{13} \cosh m_3 x_3 + g_1 m_3 \sinh m_3 x_3) R_{28} + (i\xi g_1 \alpha_{14} \cosh m_4 x_3 + g_1 m_4 \sinh m_4 x_3) R_{31} \\
L_{18} &= (i\xi g_1 \alpha_{11} \cosh m_1 x_3 + g_1 m_1 \sinh m_1 x_3) R_{23} + (i\xi g_1 \alpha_{12} \cosh m_2 x_3 + g_1 m_2 \sinh m_2 x_3) R_{26} + \\
&(i\xi g_1 \alpha_{13} \cosh m_3 x_3 + g_1 m_3 \sinh m_3 x_3) R_{29} + (i\xi g_1 \alpha_{14} \cosh m_4 x_3 + g_1 m_4 \sinh m_4 x_3) R_{32}
\end{aligned} \tag{69}$$

UNIQUE CASES

(i) For normal force $F_{20} = F_{30} = 0$ yield

$$(\widehat{u}_1, \widehat{u}_3, \widehat{t}_{33}, \widehat{t}_{31}, \widehat{T}, \widehat{N}) = \frac{1}{\Delta} ((L_1, L_4, L_{13}, L_{16}, L_7, L_{10},) \widehat{F}_1(\xi, p)) \tag{70}$$

where $\widehat{F}_1(\xi, p)$ is given by equation (46) and (49).

(ii) For thermal source $F_{10} = F_{30} = 0$ yield

$$(\widehat{u}_1, \widehat{u}_3, \widehat{t}_{33}, \widehat{t}_{31}, \widehat{T}, \widehat{N}) = \frac{1}{\Delta} ((L_2, L_5, L_{14}, L_{17}, L_8, L_{11},) \widehat{F}_2(\xi, p)) \tag{71}$$

where $\widehat{F}_2(\xi, p)$ is given by equation (47)

(iii) For carrier density source $F_{10} = F_{20} = 0$ yield

$$(\widehat{u}_1, \widehat{u}_3, \widehat{t}_{33}, \widehat{t}_{31}, \widehat{T}, \widehat{N}) = \frac{1}{\Delta} ((L_3, L_6, L_{15}, L_{18}, L_9, L_{12},) \widehat{F}_3(\xi, p)) \tag{72}$$

where $\widehat{F}_3(\xi, p)$ is given by equation (48)

LIMITING CASES

a) If $\tau_T = 0$ and $m_o = 1$ in equations (63)-(68) we obtain the corresponding expressions for single phase lag parameter.

b) If $m_o = 1, 0 < \tau_T < \tau_q$ in equations (63)-(68) attain the related expressions of photothermoelastic with dual phase lag.

c) If $\tau_q = \tau_o > 0, \tau_T = m_o = 0$ in equations (63)-(68) recover the corresponding expressions for one relaxation time.

- d) If $\tau_T = \tau_q = 0$ in equation (63)-(68) yields the expressions for photothermoelastic medium.
- e) If $\gamma_1 = \gamma_3 = 0, E_g = 0$ and $D_1^* = D_3^* = 0$ in equations (63)-(68) determines the expressions for orthotropic thermoelastic material.
- f) If $C_{11} = C_{33} = \lambda + 2\mu, C_{13} = \lambda, C_{55} = \mu, \alpha_{1t} = \alpha_{3t} = \alpha_t, \gamma_{1d} = \gamma_{3d} = \gamma_n, D_1 = D_3 = D_e$ and
- g) $K_{11} = K_{33} = K$, we obtain the desired results for normal stress and thermal distribution (without N) with the change values of equation (30) where m_1, m_2 and m_3 be the roots of characteristic equation $D^6 + R_{33}D^4 + R_{34}D^2 + R_{35} = 0$ with general solution

$(\widehat{u}_1, \widehat{u}_3, \widehat{T}) = \sum_{j=1}^3 (1, a_j, b_j) C_j \cosh m_j x_3$ and the coupling parameters are

$$a_j = \sum_{j=1}^3 \frac{R_{39}m_j^3 + R_{40}m_j}{R_{36}m_j^4 + R_{37}m_j^2 + R_{38}} \quad \text{and} \quad b_j = \sum_{j=1}^3 \frac{R_{41}m_j^2 + R_{42}}{R_{36}m_j^4 + R_{37}m_j^2 + R_{38}}$$

NUMERICAL RESULTS AND DISCUSSION:

For the numerical calculations we take material constants for an isotropic Silicon (Si) material given by (Hobiny and Abbas[26]).

$\lambda = 3.64 \text{ N/m}^2, \mu = 5.46 \text{ N/m}^2, \gamma_t = 6.55 \text{ N/m}^2 \text{K}, \gamma_n = -0.0195 \text{ N/m}^2, \rho = 0.2330 \text{ kg/m}^3, T_0 = 300 \text{ K}, T_p = 2 \text{ ps}, K = 150 \text{ w/mk}, E_g = 1.11 \text{ eV}, C_e = 695 \text{ J/kg K}, \tau = 5 \text{ s}, \tau_o = 0.2 \text{ ps}, d_n = -9 \text{ m}^3, D_e = 2.5 \text{ m}^2/\text{s}$

For orthotropic material we have taken following values

$C_{11} = 19.45 \text{ N/m}^2, C_{13} = 6.41 \text{ N/m}^2, C_{33} = 16.57 \text{ N/m}^2, C_{55} = 7.96 \text{ N/m}^2, \alpha_{1t} = 3.25 \text{ N/m}^2 \text{K}, \alpha_{3t} = 3.10 \text{ N/m}^2 \text{K}, \gamma_{1d} = -0.029715 \text{ m}^3, \gamma_{3d} = -0.02714 \text{ m}^3, \rho = 0.2328 \text{ kg/m}^3, T_0 = 300 \text{ K}, T_p = 2 \text{ ps}, K_{11} = 192 \text{ w/mk}, K_{33} = 190 \text{ w/mk}, E_g = 1.11 \text{ eV}, C_e = 710 \text{ J/kg K}, \tau = 5 \text{ s}, D_1^* = 4.0 \text{ m}^2/\text{s}, D_3^* = 3.5 \text{ m}^2/\text{s}, n_o = 10^{20} \text{ m}^{-3}$

The MATLAB (R2016a) software has been used for numerical computation for the following cases:

- i. Orthotropic photothermoelastic with dual phase lag (OPTP).
- ii. Orthotropic photothermoelastic with LS theory (OPTL).
- iii. Orthotropic photothermoelastic without dual phase lag (OPT).
- iv. Isotropic photothermoelastic with dual phase lag (IPTP).

Figures (1.1)-(1.3) and (1.13-1.15) represents uniformly distributed normal force (UDF), figures (1.4)-(1.6) and (1.16)-(1.18) represents linearly distributed normal force (LDF), figures (1.7)-(1.9) and (1.19)-(1.21) represents thermal source (TS), and figures (1.10)-(1.12) and (1.22)-(1.23) represents carrier density source (CDS). In all the figures, solid line correspond to OPTP for $\tau_T = 0.02, \tau_q = 0.04, m_o = 1$, dash line correspond to OPTL for $\tau_T = 0, \tau_o = 0.04, m_o = 0$, dotted line correspond to OPT for $\tau_T = \tau_q = 0$ and dash cum dot line correspond to IPTP for $\tau_T = 0.02, \tau_q = 0.04, m_o = 1$.

Case-I: Figure (1.1)-(1.12) depict the variations of all field variables with plate length x_1 on the plane $x_3 = 1$.

Normal force (UDF):

Figure 1.1 depicts trend of normal stress t_{33} vs x_1 . Near the loading point, t_{33} shows decreasing trend for all the cases whereas far away from it t_{33} attains increasing trend except IPTP. In the initial range of x_1 , OPT maximize the magnitude of t_{33} in comparison to OPTP, OPTL and OPT. All the curves correspond to t_{33} depict fluctuating behavior for entire range of x_1 .

Figure 1.2 displays variations of temperature distribution T vs x_1 . T shows increasing trend near the point of application of source for all cases except IPTP, whereas away from it T gets increasing trend for all the cases. The magnitude of T enhanced due to one relaxation time as compare to other cases. The trend and variation of OPT and OPTP are similar with difference in magnitude.

Figure 1.3 demonstrates trend of carrier density distribution N vs x_1 . Initially, for the limited range of x_1 , N

depicts increasing trend for all curves except IPTP. Phase lag enhanced the magnitude of N in contrast to OPTL, OPT and IPTP. For intermediate values of x_1 , N follows oscillatory behavior for all cases.

Normal force (LDF):

Figure 1.4 shows trend of normal stress t_{33} vs x_1 . Near the point of loading t_{33} depicts the decreasing trend for all cases. In the initial range of x_1 , the magnitude of t_{33} is higher due to phase lag in comparison to other cases. The values of t_{33} determine a bell shaped curve for IPTP in the range $5 \leq x_1 \leq 13$.

Figure 1.5 displays variation of temperature distribution T vs x_1 . For initial values of x_1 , T shows decreasing trend for OPTP, OPTL and IPTP except OPT. The magnitude of T is higher for OPT in comparison to other cases. In the range $11 \leq x_1 \leq 20$, phase lag depicts a bell shape curve correspond to T.

Figure 1.6 demonstrates variation of carrier density distribution N vs x_1 . All the curves for OPTP, OPTL, OPT and IPTP corresponds to N display decreasing and increasing trend near and away from the loading point. N attains maximum value for IPTP at the initial values of x_1 , whereas phase lag enhance the magnitude of N in the finite domain of x_1 .

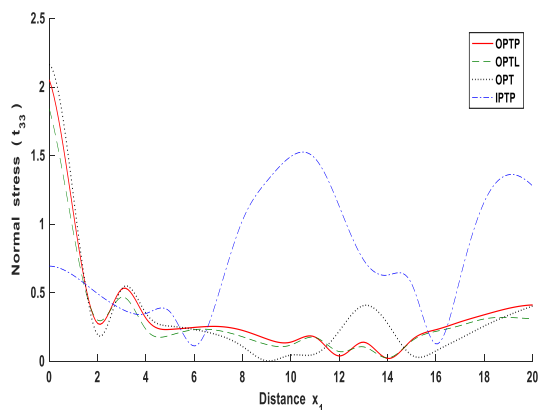


Figure 1.1 Profile of t_{33} vs x_1 (UDF)

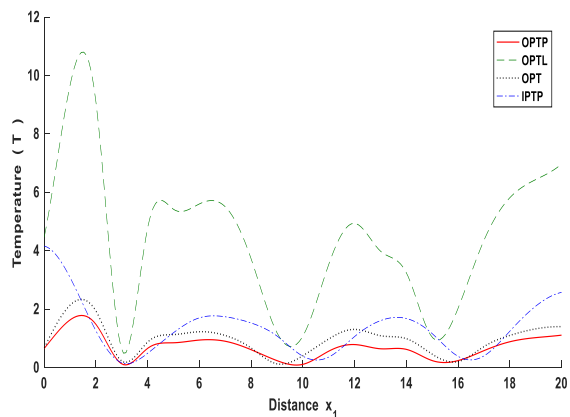


Figure 1.2 Profile of T vs x_1 (UDF)

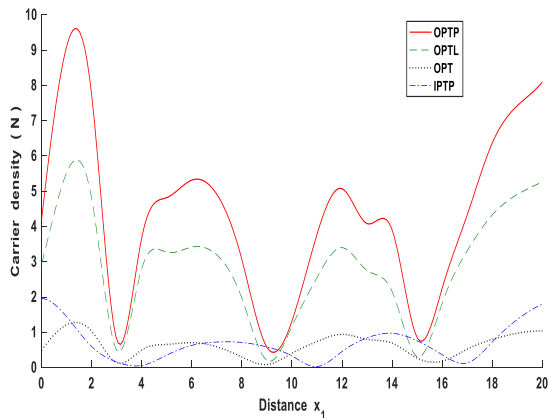


Figure 1.3 Profile of N vs x_1 (UDF)

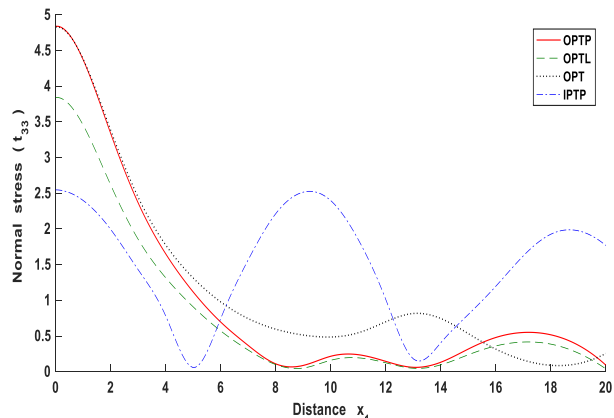


Figure 1.4 Profile of t_{33} vs x_1 (LDF)

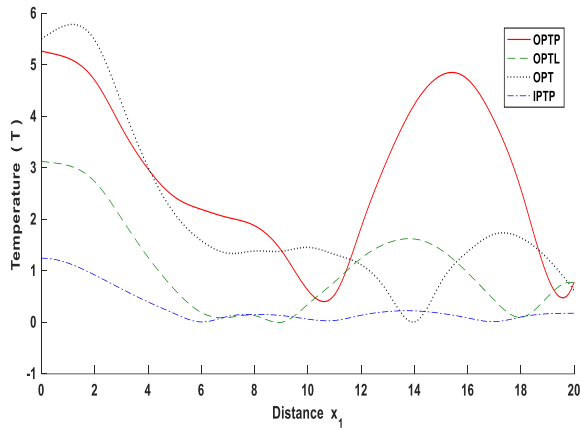


Figure 1.5 Profile of T vs x_1 (LDF)

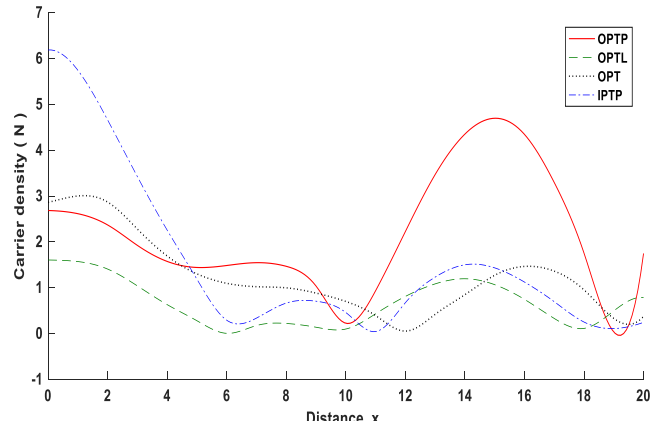


Figure 1.6 Profile of N vs x_1 (LDF)

Thermal Source:

Figure 1.7 displays trend of normal stress t_{33} vs x_1 . Initially, the values of t_{33} depict decreasing trend for OPTP, OPTL and OPT. Near the point of loading, the magnitude of t_{33} is higher due to phase lag in comparison to other cases. The behavior of t_{33} shows a parabolic curve for IPTP in the range $10 \leq x_1 \leq 16$. The trend and variation of OPTL and OPTP are similar with difference in magnitude of t_{33} .

Figure 1.8 shows trend of temperature distribution T vs x_1 . The values of T decrease initially for OPTL and OPT, whereas increase for OPTP and IPTP in limited range of x_1 . All the curves for OPTP, OPTL, OPT and IPTP correspond to T shows oscillatory behavior in the range $2 \leq x_1 \leq 20$. Phase lag enhances the magnitude of T in the range $10 \leq x_1 \leq 16$.

Figure 1.9 demonstrates variation of carrier density distribution N vs x_1 . One relaxation time enhances the magnitude of N near the loading point in comparison to other cases. All the curves for OPTP, OPTL, OPT and IPTP correspond to N follow oscillatory trend for the range $4 \leq x_1 \leq 20$.

Carrier density source:

Figure 1.10 displays trend of normal stress t_{33} vs x_1 . Phase lag enhances the magnitude of t_{33} in the range $1 \leq x_1 \leq 4$ in comparison to other cases. Away from the point of application of the source t_{33} attains increasing trend for all the cases. All curves for OPTP, OPTL, OPT and IPTP refers to t_{33} shows fluctuating behavior for the entire range $4 \leq x_1 \leq 20$.

Figure 1.11 shows trend of temperature distribution T vs x_1 . T attains decreasing trend for all cases except OPTL in initial range of x_1 . The magnitude of T is higher due to one relaxation time in comparison to other cases. For all cases, T depict oscillatory trend for the intermediate values of x_1 .

Figure 1.12 depicts trend of carrier density distribution N vs x_1 . Due to phase lag, the magnitude of N is maximum for the entire domain of x_1 , except at two points in contrast to other cases. All the curves for OPTP, OPTL, IPTP and OPT corresponds to N follows fluctuating behavior for the whole range of x_1 .

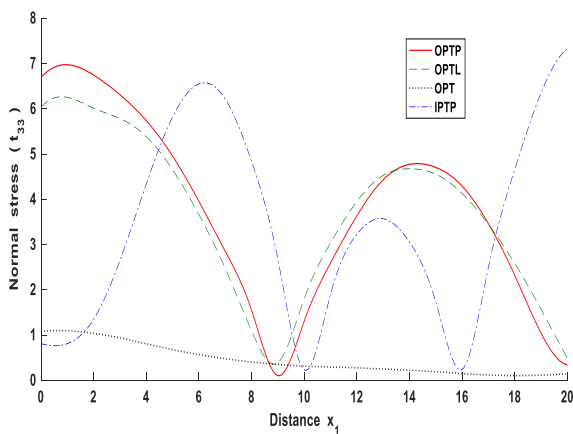


Figure 1.7 Profile of t_{33} vs x_1 (TS)

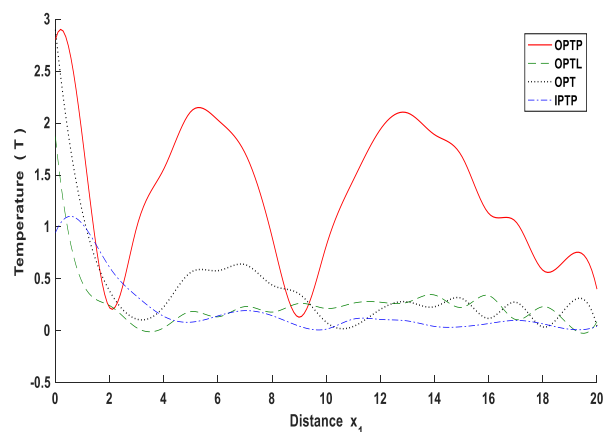


Figure 1.8 Profile of T vs x_1 (TS)

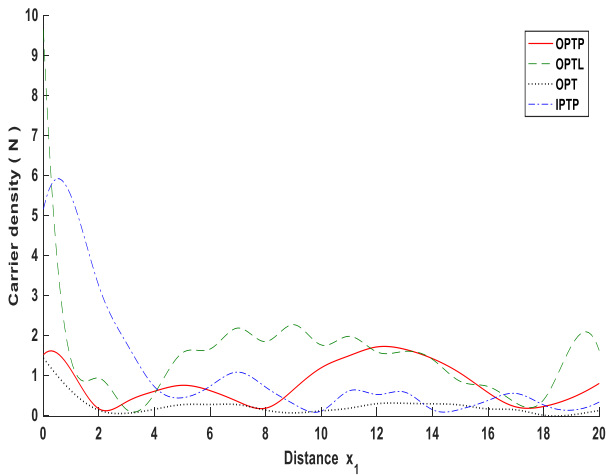


Figure 1.9 Profile of N vs x_1 (TS)

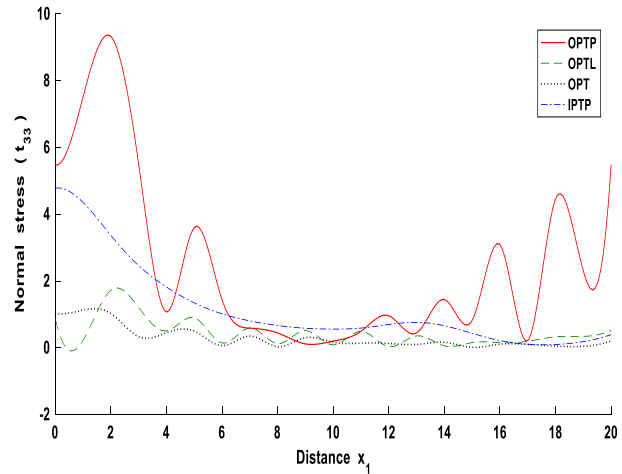


Figure 1.10 Profile of t_{33} vs x_1 (CDS)

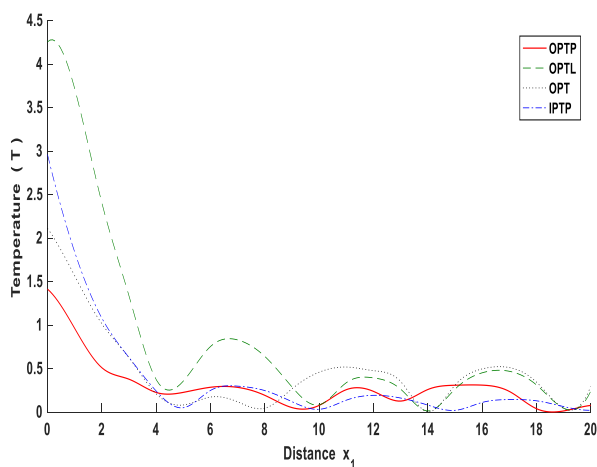


Figure 1.11 Profile of T vs x_1 (CDS)

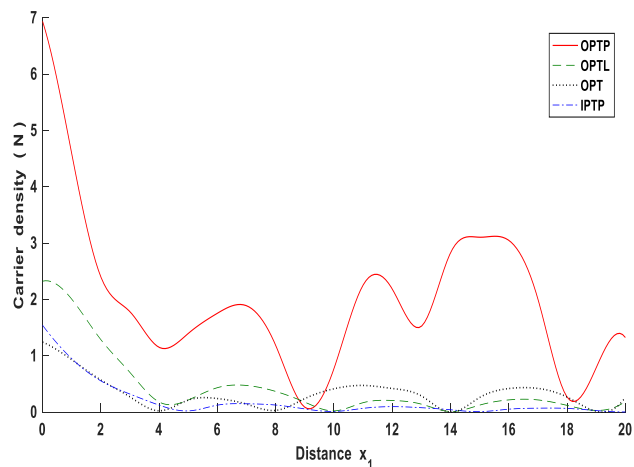


Figure 1.12 Profile of N vs x_1 (CDS)

Case-II: Figure (1.13)-(1.24) show the variations of all field variables with plate thickness x_3 on the plane $x_1 = 1$.

Normal force (UDF):

Figure 1.13 depicts trend of normal stress t_{33} vs d . In the range $|d| \leq 5$, t_{33} shows oscillatory trend for all the cases. The magnitude of t_{33} is higher at the middle point of the plate for IPTP as compare to OPTP, OPTL and OPT. The value of t_{33} reduces just near the edges ($d = -5$ and $d = 5$) for all the cases. The behavior and variation of OPT and OPTP is similar although a difference in their magnitude is noticed.

Figure 1.14 displays trend of temperature distribution T vs d . For all cases, behavior of T is oscillatory for the intermediate values of d . The magnitude of T remains higher due to one relaxation time except at two points, in comparison to rest of the cases. The values of T decrease just near the edges ($d = -5$ and $d = 5$), for all the cases. The trend of T for OPTL and IPTP is opposite in comparison to OPTP and OPT at the middle point of the plate.

Figure 1.15 demonstrates trend of carrier density distribution N vs d . N shows fluctuating behavior for all the cases in whole range of d . Due to phase lag the magnitude of N is higher at $d = -1$ and $d = 1$ in contrast to OPTL, OPT and IPTP. The magnitude of N displays decreasing trend just near the boundaries ($d = -5$ and $d = 5$) for all the cases.

Normal force (LDF):

Figure 1.16 shows trend of normal stress t_{33} vs d . t_{33} gets maxima at the middle point of the plate for OPTP in contrast to OPTL, OPT and IPTP. The magnitude of t_{33} decreases for IPTP and increase for OPTP, OPTL and OPT near the edges ($d = -5$ and $d = 5$). The trend and variation of OPT and OPTP is similar while a difference in magnitude is observed.

Figure 1.17 displays trend of temperature distribution T vs d . T depicts oscillatory trend for all the cases in the range $-5 \leq d \leq 5$. The magnitude of T is higher at $d = -1$ and $d = 1$ in the absence of phase lag as compare to other cases. Just adjacent the boundaries the magnitude of T decrease for IPTP and increase for OPTP, OPTL and OPT. Variation and behavior of T for model OPTP and OPT are similar.

Figure 1.18 demonstrates trend of carrier density distribution N vs d . In all the cases magnitude of N shows fluctuating nature for the entire range of d . The value of N is higher at the middle point of the plate for model IPTP as compare to OPTP, OPTL and OPT. The magnitude of N decreases for IPTP and increases for OPTP, OPTL and OPT near the edges ($d = -5$ and $d = 5$).

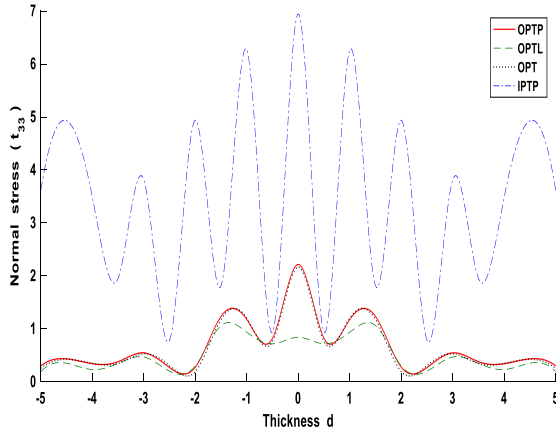


Figure 1.13 Profile of t_{33} vs d (UDF)

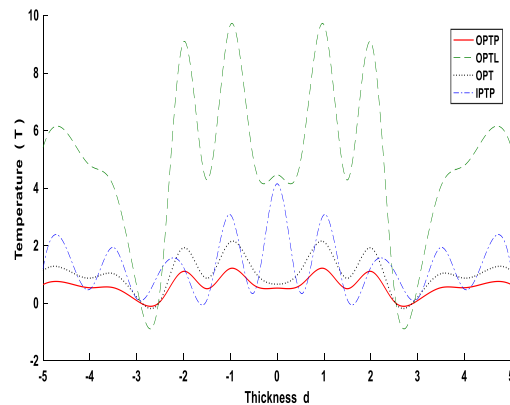


Figure 1.14 Profile of T vs d (UDF)

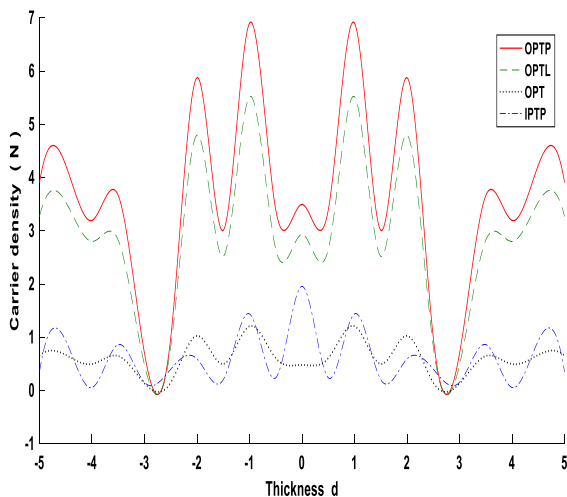


Figure 1.15 Profile of N vs d (UDF)

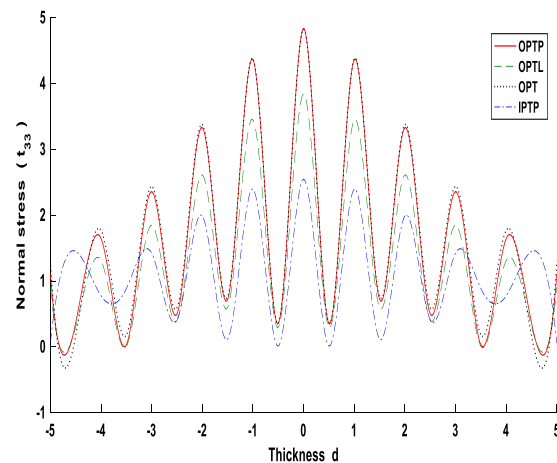


Figure 1.16 Profile of t_{33} vs d (LDF)

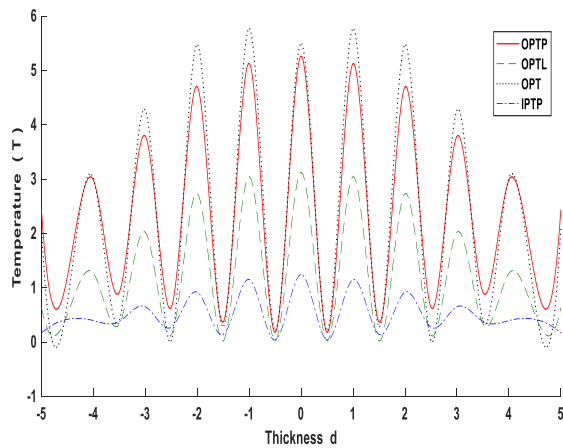


Figure 1.17 Profile of T vs d (LDF)

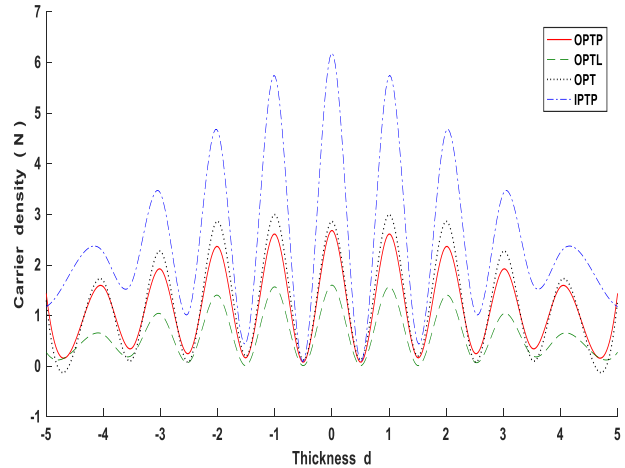


Figure 1.18 Profile of N vs d (LDF)

Thermal Source:

Figure 1.19 shows trend of normal stress t_{33} vs d . The behavior and variation of t_{33} , for IPTP are opposite to OPTP, OPTL and OPT for all values of d . The values of t_{33} attain oscillatory trend for all the cases in the range $|d| \leq 5$. Phase lag enhanced the magnitude of t_{33} at $d = -1$ and $d = 1$. The behavior and variation of t_{33} for OPTP, OPT and IPTP are similar with difference in their magnitude.

Figure 1.20 displays trend of temperature distribution T vs d . T depicts oscillatory trend for all the cases in the range $|d| \leq 5$. The magnitude of T is higher at the middle of the plate for OPTP as compare to other cases. The values of T decrease for OPTL and IPTP and increase for OPTP and OPT, near the edges ($d = -5$ and $d = 5$).

Figure 1.21 depicts trend of carrier density distribution N vs d . In all the cases, the magnitude of N shows fluctuating behavior in the bounded range of d . N attains maxima in the range $-1 \leq d \leq 1$, for OPTL. Near the boundaries the values of N decrease for all cases except OPT.

Carrier density source:

Figure 1.22 shows trend of normal stress t_{33} vs d . t_{33} shows oscillatory trend for all the cases in the range $-5 \leq d \leq 5$. The magnitude of t_{33} is higher at the middle of the plate for IPTP as compare to OPTL, OPTP and OPT. The magnitude of t_{33} decrease for OPTP, whereas increase for OPTL, OPT and IPTP near the edges ($d = -5$ and $d = 5$).

Figure 1.23 demonstrates trend of temperature distribution T vs d . T depicts fluctuating trend for all the cases for the intermediate values of d . The magnitude of T is higher at the middle point of the plate, due to one relaxation time. The values of T decrease for OPTP, OPTL and IPTP, however increase for OPT near the boundary points ($d = -5$ and $d = 5$).

Figure 1.24 depicts trend of carrier density function N vs d . In all the cases magnitude of N shows oscillatory behavior in the range $-5 \leq d \leq 5$. One relaxation time enhances the magnitude of N as compare to IPTP, OPTP and OPTL and increase for OPT near the edges ($d = -5$ and $d = 5$).

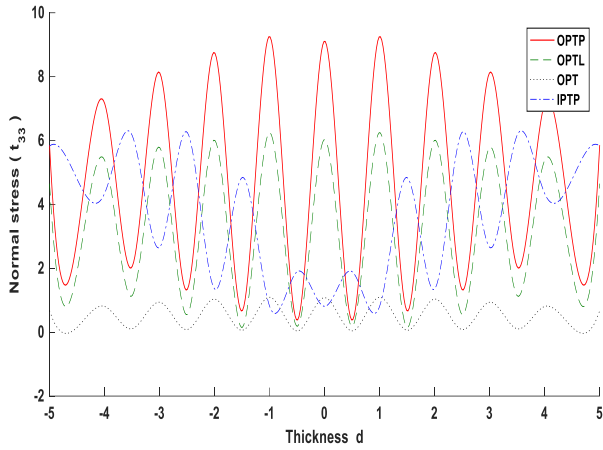


Figure 1.19 Profile of t_{33} vs d (TS)

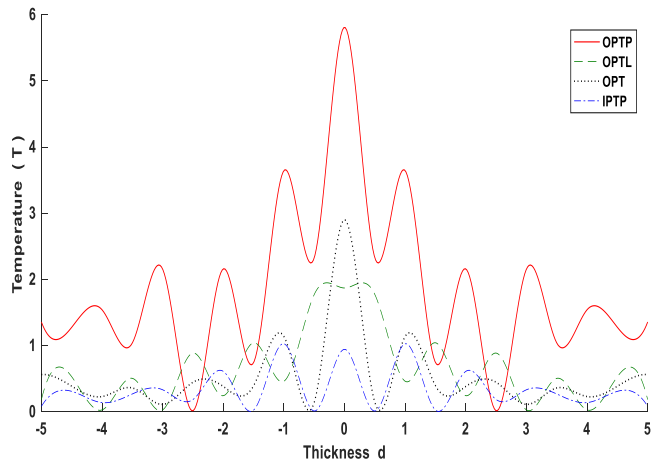


Figure 1.20 Profile of T vs d (TS)

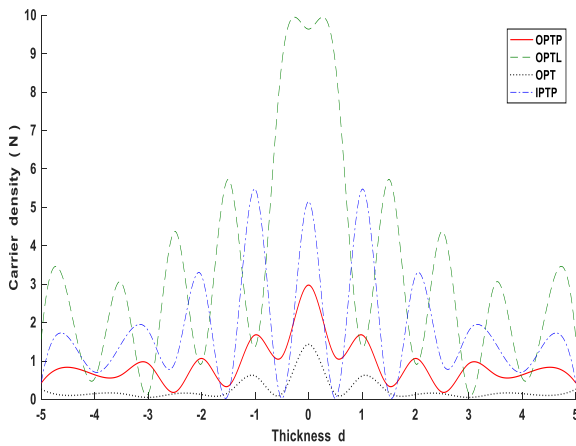


Figure 1.21 Profile of N vs d (TS)

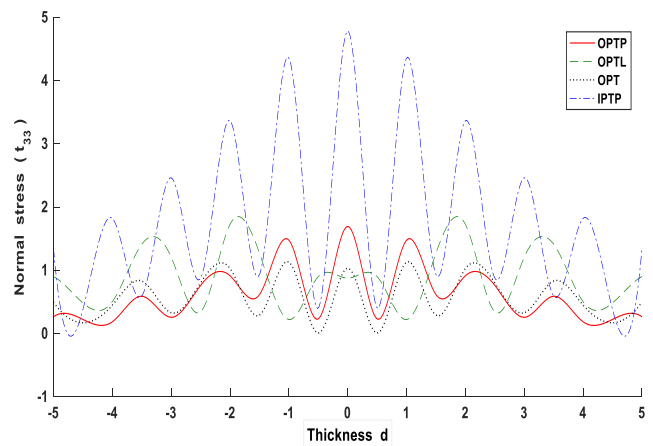


Figure 1.22 Profile of t_{33} vs d (CDS)

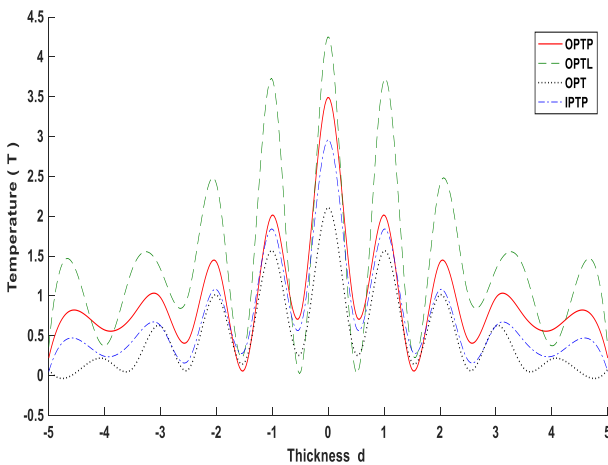


Figure 1.23 Profile of T vs d (CDS)

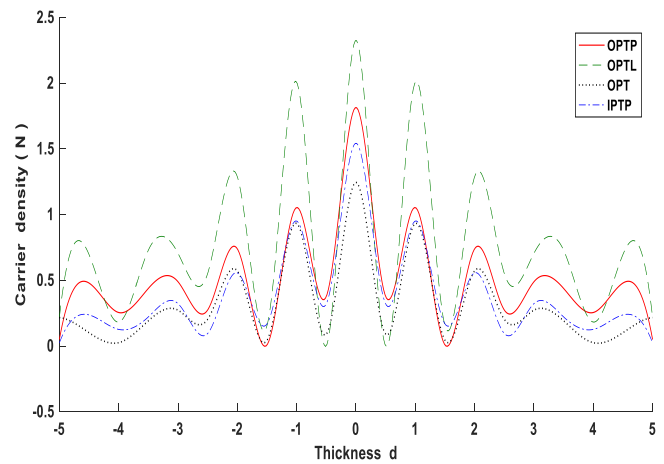


Figure 1.24 Profile of N vs d (CDS)

CONCLUSIONS

In this paper a new model of orthotropic photothermoelastic material has been established due to various loadings (thermomechanical and carrier density source). Laplace and Fourier transform are used to solve the problem. Specific types of sources are taken to demonstrate the utility of the problem. Numerical conversion technique has been employed to obtain the transformed expressions into the physical domain and presented in the form of figures. From the numerical results the following conclusions are made

1. For normal force (UDF), in the initial range of x_1 , magnitude of t_{33} for OPT is higher as compare to other cases. The behavior and variation of t_{33} for OPTP, OPTL and OPT are similar with difference in

magnitude.

2. For normal force (UDF), one relaxation time enhances the value of T, near the application of the source. All the curves correspond to T attains increasing trend away from the loading point.
3. For normal force (UDF), phase lag maximize the value of N, for the initial range of x_1 , in comparison to other cases.
4. For normal force (LDF), near the point of loading, the magnitude of t_{33} higher due to phase lag. For the starting values of x_1 , negligible difference in values of t_{33} is observed for OPTP and OPT.
5. For normal force (LDF), in the bounded range of x_1 , the magnitude of T increases due to absence of phase lag. In the range $11 \leq x_1 \leq 20$, phase lag depicts a bell shape curve correspond to T.
6. For normal force (LDF), N attains higher value for IPTP in comparison to other cases.
7. For thermal source, near the application of the source phase lag maximize the values of t_{33} . The behavior of t_{33} is parabolic in nature for the range $10 \leq x_1 \leq 16$.
8. For thermal source, phase lag enhances the magnitude of T, near the loading point.
9. For thermal source, one relaxation time increases the magnitude of N, near the application of the source, in comparison to other cases.
10. For carrier density source, t_{33} have maxima in the bounded domain of x_1 for OPTP.
11. For carrier density source, one relaxation time attains higher magnitude of T near the loading point. T depicts decreasing trend for all cases, in the initial range of x_1 . Oscillatory behavior for all the curves related to T is observed in the range $4 \leq x_1 \leq 20$.
12. For carrier density source, the magnitude of N is higher for the whole domain of x_1 , due to phase lag, except at two points in contrast to other cases.
13. For normal force (UDF), the magnitude of t_{33} is higher at the middle point of the plate for IPTP as compare to other cases. Variation and trend are similar for OPT and OPTP corresponds to t_{33} with change in magnitude.
14. For normal force (UDF), One relaxation time enhanced the magnitude of T at $d = -1$ and $d = 1$, whereas the values of T decrease just near the edges ($d = -5$ and $d = 5$), for all the cases.
15. For normal force (UDF), t_{33} gets maxima at the middle point of the plate for OPTP in contrast to OPTL, OPT and IPTP.
16. For normal force (LDF), t_{33} attains maxima for intermediate values of d, due to phase lag.
17. For normal force (LDF), in the absence of phase lag T gets maximum magnitude at $d = -1$ and $d = 1$. T attains lowest values for IPTP for the whole range of d.
18. For normal force (LDF), the value of N enhances in absence of orthotropy.
19. For thermal source, phase lag boost the magnitude of t_{33} at $d = -1$ and $d = 1$. t_{33} for IPTP, behave opposite in comparison to other cases, for the intermediate values of d.
20. For thermal source, the magnitude of T remains higher at the middle of the plate for OPTP as compare to rest of the cases.
21. For thermal source, N shows fluctuating behavior for the bounded range of d.
22. For carrier density source, in absence of orthotropy, t_{33} attain maxima at the middle of the plate.
23. For carrier density source, T and N determine the higher magnitude for one relaxation time, in comparison to other cases.
24. All the curves for OPTP, OPTL, OPT and IPTP corresponds to t_{33} , T and N w.r.t. thickness, are symmetric around the middle point of the plate.

It is concluded that normal stress, temperature distribution and carrier density distribution show a fluctuating behavior in presence and absence of orthotropy, phase lag and one relaxation time. Non-uniform pattern of curves is followed by the resulting quantities for normal force over UDF and LDF, thermal source and carrier

density source with respect to distance. Oscillatory behavior is observed for normal force, thermal source and carrier density function with respect to thickness of the plate.

REFERENCES

- [1] Mandelis, A., "Photoacoustic and Thermal wave Phenomena in Semiconductors" Elsevier Science, North- Holland, New York, 1987.
- [2] Almond, D.P., and Patel, P.M., "Photothermal Science and Techniques" Chapman and Hall, London, 1996.
- [3] Mandelis, A., and Michaelian, K.H., "Photoacoustic and Photothermal Science and Engineering" Optical Engineering, 1997; 36(2):301-302.
- [4] Abbas A., "A dual phase lag model on photothermal interaction in an unbounded semiconductor medium with cylindrical cavity", IJCM Science and Engineering, 2016; 5(3):1650016(13).
- [5] Lotfy, Kh., "The elastic wave motions for a photothermal medium of a dual-phase-lag model with an internal heat source and gravitational field", Canadian Journal of Physics, 2016; 94: 400-409.
- [6] Lotfy, Kh., "Photothermal waves for two-temperature with a semiconducting medium under using a dual-phase-lag model and hydrostatic initial stress", Waves Random Complex Media, 2017a; 27(3): 482-501.
- [7] Lotfy, Kh., "A novel solution of fractional order heat equation for photothermal waves in a semiconductor medium with a spherical cavity", Chaos, Solitons and Fractals, 2017 b ; 99:233- 242.
- [8] Lotfy, Kh., Kumar, R., Hassan, W., and Gabr, M., "Thermomagnetic effect with microtemperature in a semiconducting photothermal excitation medium", Appl. Math Mech.-Engl. Ed, 2018; 39: 783–796.
- [9] Hobiny, A., and Abbas, A., "Analytical solutions of photo-thermo-elastic waves in a non-homogeneous semiconducting material", Results in Physics (Elsevier), 2018; 10:385-390.
- [10] Jahangir, A., Tanvir, F., and Zenkour, A.M., "Reflection of photothermoelastic waves in a semiconductor material with different relaxations", Indian Journal of Physics 2020 ; 95:51-59.
- [11] Zenkour, A.M., "Exact coupled solution for photothermal semiconducting beams using a refined multi-phase-lag theory", Optics and Laser Technology, 2020; 128: 106233.
- [12] Alzahrani, F., and Abbas, A., "The Effect of a Hyperbolic Two-Temperature Model with and without Energy Dissipation in a Semiconductor Material", Mathematics, 2020a; 8(10):1711.
- [13] Alzahrani, F., and Abbas, A., "Photo-Thermal Interactions in a Semiconducting Media with a Spherical Cavity under Hyperbolic Two-Temperature Model", Mathematics, 2020b, doi.org/10.3390/math8040585.
- [14] Saeed, T., "Photo-thermo-elastic interaction in a semiconductor material upon hyperbolic two-temperature and thermal relaxation times", Waves in Random and Complex Media, 2021, doi.org/10.1080/17455030.2021.1876961.
- [15] Abbas, I., Saeed, T., and Alhothuali, M., "Hyperbolic Two-Temperature Photo-Thermal Interaction in a Semiconductor Medium with a Cylindrical Cavity", Silicon, 2021; 13:1871–1878.
- [16] Hobiny, A., Alzahrani, S., and Abbas, A., "A study on photo-thermo-elastic wave in a semiconductor material caused by ramp-type heating", Alexandria Engineering Journal, 2021; 60(2):2033-2040.
- [17] Alzahrani, F., and Abbas, A., "A numerical solution of nonlinear DPL bioheat model in biological tissue due to laser irradiations", Indian J Phys, 2021, doi.org/10.1007/s12648-020-01988-w.
- [18] Zakaria, K., Sirwah, M., Abouelregal, A., and Rashid, A., "Establishing a memory-dependent photothermoelastic model according to the dual phase lag model on a cylindrical body rotating in an initial magnetic field", Authorea, 2021a, doi.org/10.22541/au.161193018.80757142/v1.
- [19] Zakaria, K., Sirwah, M.A., and Abouelregal, A.E., "Photo-Thermoelastic Model with Time-Fractional of Higher Order and Phase Lags for a Semiconductor Rotating Materials", Silicon, 2021b; 13: 573–585.
- [20] Tzou, D. Y., "A unified approach for heat conduction from macro-to-micro-scales", Journal Heat Transfer, 1995; 117(1):8-16.

- [21] Todorovic, D.M., " Plasma, thermal and elastic waves in semiconductors" Review of Scientific Instruments, 2003; 74(1): 582-585.
- [22] Todorovic, D.M., "Plasmaelastic and thermoelastic waves in semiconductors" In Journal de Physique archives, 2005;125(4),551-555.
- [23] Lord, H.W.,and Shulman, Y., "A generalized dynamical theory of thermoelasticity", J. Mech. Phys. Solids, 1967; 15: 299–309.
- [24] Dhaliwal, R.S.,and Singh A., "Dynamic Coupled Thermoelasticity",SIAM Review, 1983;25(1): 126-127.
- [25] Slaughter, W.S., "The Linearized Theory of Elasticity",Birkhauser, 2002.
- [26] Hobiny, A.,and Abbas, A., " A study on photothermal waves in an unbounded semiconductor medium with cylindrical cavity", Mech Time Depend Mater, 2016;21(1):61-72.